Subdivide and Conquer: Adapting Non-manifold Subdivision Surfaces to Surface-Based Representation and Reconstruction of Complex Geological Structures

s.Mohammad Moulaeifard[1], Florian Wellmann[1,2], Simon Bernard[1], Miguel de la Varga[2] , David Bommes[3]

[1]Computational Geoscience and Reservoir Engineering, RWTH Aachen University, Aachen, Germany

[2]Terranigma Solutions GmbH, Aachen, Germany

[3]Computer Graphics Group, Institute of Computer Science, University of Bern, Bern, Switzerland

Correspond Author: s.Mohammad Moulaeifard (mohammad.moulaeifard@cgre.rwth-aachen.de)

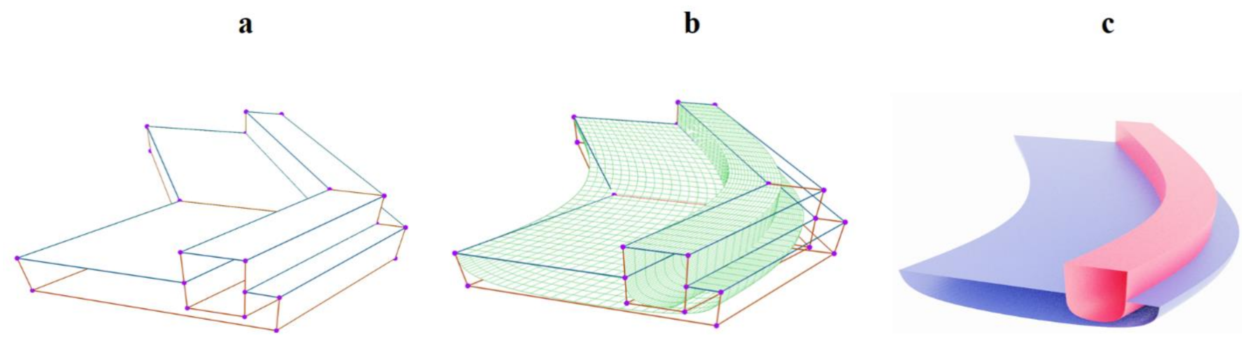

Fig. 1 Representation of the procedure to generate a geological structure with non-manifold topology by using a surface-based non-manifold subdivision surface method from a coarse mesh: **a** Control mesh with the control points (purple) and the edges with different crease sharpness values (blue and red). **b** Smooth and subdivided mesh generated by repeatedly applying a subdivision surface algorithm modified by control points (purple). **c** Rendered version of the final mesh.

Abstract

Methods from the field of Computer Graphics are the foundation for the representation of geological structures in the form of geological models. However, as many of these methods have been developed for other types of applications, some of the requirements for the representation of geological features may not be considered and the capacities and limitations of different algorithms are not always evident. In this work, we, therefore, review surface-based geological modelling methods from both a geological and computer graphics perspective. Specifically, we investigate the use of NURBS (Non-Uniform Rational B-Splines) and subdivision surfaces, as two main parametric surface-based modelling methods, and compare the strengths and weaknesses of both approaches. Although NURBS surfaces have been used in geological modelling, subdivision surfaces as a standard method in the animation and gaming industries have so far

received little attention – even if subdivision surfaces support arbitrary topologies and watertight modelling, two aspects that make them an appealing choice for complex geological modelling. Watertight modelling is a type of modelling in which the surfaces of the model have sealed interactions with all surrounding surfaces, resulting in the generation of closed volumes. Watertight models are, therefore, an important basis for subsequent process simulations based on these models.

Many complex geological structures require a combination of smooth and sharp edges. Investigating subdivision schemes with semi-sharp creases is therefore an important part of this paper, as semi-sharp creases characterize the resistance of a mesh structure to the subdivision procedure. Moreover, non-manifold topologies, as a challenging concept in complex geological and reservoir modelling, are explored, and the subdivision surface method, which is compatible with non-manifold topology is described.

Finally, solving inverse problems by fitting the smooth surfaces to complex geological structures is investigated with a case study. The fitted surfaces are watertight, controllable with control points, and topologically similar to the main geological structure. Also, the fitted model can reduce the cost of modelling and simulation by using a reduced number of vertices in comparison to the complex geological structure.

Keywords Surface-based modelling. Subdivision surfaces. Non_manifold topology. Approximation of geological structures. Grid free. NURBS.

1 Introduction

Surface representation is one of the common concepts between geology and computer graphics. According to Botsch et al. (2010), implicit and parametric representations can be considered as the two main types of surface representations, where in both types, the surface is defined by a specific function; "implicit surfaces" are defined by a scalar-valued function, and the aim is to find a zero level set, whereas a "parametric surface" is defined by a vector-valued function, and the aim is to convert the 3D models to 2D models in the parametric domain. A parametric representation has advantages over an implicit representation in the direct representation of surfaces and it can present details in a more compact and modifiable form but at the cost of requiring more effort for calculating spatial queries (Botsch et al. 2010).

Similar to applications in computer graphics, parametric surface-based geological and reservoir representations are defined by the surrounding surfaces (Jacquemyn et al. 2019; Wellmann and Caumon 2018; Graham et al. 2015a, b; Jackson et al. 2015, 2013; Deveugle et al. 2011; Caumon et al. 2009, De Kemp 1999). In contrast to grid-based implicit geomodeling, one of the key advantages of parametric surface-based methods is that most of the critical details of the model, such as heterogeneity, will be well maintained since there is no need to dispense the features over the grid cells and therefore to obtain the "averaged value" within the cells (Jacquemyn et al. 2019; Ruiu et al. 2016; Pyrczetal. 2009; Zhang et al. 2009). In addition to implicit and parametric surface-based models, previous studies have investigated hybrid methods (Ruiu et al. 2016; Hassanpour et al. 2013; Pyrcz et al. 2009). Although hybrid approaches lead to more acceptable and faithful results, the requirement of a high-resolution grid cannot be neglected (Jacquemyn et al. 2019).

From a computer graphics point of view, spline surfaces and subdivision surfaces are two types of parametric surface-based representations (Botsch et al. 2010). Spline surfaces are the usual standard for computer-aided design (CAD), while subdivision surfaces are primarily used in computer gaming, animation and the film industry (Cashman 2010, Botsch et al. 2010). Generally, subdivision surfaces and NURBS both yield controllable freeform representations, but in different ways; NURBS emphasise the "smooth manipulation" of the model, whereas subdivision surfaces tend to release the model from "topological limitations (constraints)" (Cashman 2010) and enable surfaces with "arbitrary topology" (Botsch et al. 2010). The term topology refers to the connection between different elements of the model, and in geological modelling, it is a vital constraint for most geological procedures and actions, e.g., fluid flow, heat transfer and deformation (Burns 1975; Deutsch 1998; Jones 1989; Mallet 1997, Thiele et al. 2016).

Jacquemyn et al. (2019, 2016) hold the view that using NURBS in geology and reservoir modelling has been limited until now because modelling in this field was initially dominated by grid-based modelling methods. Previous studies using NURBS for geological, reservoir and fracture modelling showed that NURBS had been used for various goals in this context (Jacquemyn et al. 2019, 2016; Börneretal. 2015; Zehner et al. 2015; Florez et al. 2014; Corbett et al. 2012; Geiger and Matthäi 2012; Caumon et al. 2010; Paluszny et al. 2007, De Kemp et Sprague 2003; Fisher et Wales 1992; Gjøystdal et al. 1985; de Kemp 1999; Sprague et de Kemp 2005). However, subdivision surfaces have rarely been used in geological and reservoir modelling. Chen and Liu (2012) investigated geological modelling using the subdivision surface method. Although their work deserves appreciation, the authors did not explain the practical details of this approach and offered no explanation for the distinction between using spline surfaces and subdivision surfaces in parametric surface-based geological modelling.

NURBS support "non-uniform" parametrisation by using the knot vector, which can change the degree of the curve or surface at any knot (Ruiu et al. 2016, Cashman 2010). Although the classic subdivision scheme cannot support “non-uniform” parametrisation, this scheme provides a significant benefit over NURBS by supporting watertight surfaces with arbitrary topology since it eliminates the procedure of stitching and editing different surface patches (Cashman 2010). There are solutions (methods) that exploit the advantages of both NURBS and subdivision schemes, e.g., NURBS compatible with subdivision surfaces (Cashman 2010), Non-uniform recursive subdivision Surfaces (Sederberg et al. 1998) and T-NURCCs (Non-Uniform Rational Catmull-Clark Surfaces with T-junctions) (Sederberg et al. 2003).

In reservoir modelling, NURBS “curves” have been used to represent well trajectories (Jacquemyn et al. 2019). Additionally, NURBS “surfaces” have been used for modelling sinuous channels by tensor products between two NURBS curves: one NURBS curve for defining the cross-section and one curve for the trajectory of the channel (Ruiu et al. 2016). Therefore, Non-uniform parametrisation can make NURBS suitable for modelling structures with several different meanders (curvatures) along a path (trajectory). On the other hand, subdivision surfaces have fewer difficulties in modelling watertight surface intersections, which is more beneficial for channels intersecting with each other or layers. Therefore, one possibility of taking advantage of both NURBS and subdivision surfaces in geological modelling is to use both of these methods simultaneously, e.g. for generating the meanders.

Considering the fact that the concept of cellular complexes underpins the majority of topological representations, “non-manifold surfaces” are defined as the 2D cellular complex surfaces when the vicinity of each point is not homeomorphic to an open disc (Caumon et al. 2004). Also, in a triangle mesh, an edge is called a “non-manifold” if it is incident to more than two triangles. The non-manifold structures need more complex algorithms for the representations (Rossignac and Cardoze 1999). Figure 2 shows one of the common examples of non-manifold surfaces in geological modelling, which contains three surfaces shared by one edge. Green edge and yellow vertices are non-manifold edges and vertices, respectively. From the geological modelling point of view, contacts between geological interfaces where multiple faces of the mesh are shared by one edge (e.g. intersection between faults or between faults and horizons) are common examples of non-manifold surfaces (Caumon et al. 2004). Also, complex geological structures commonly comprise multiple intersecting surfaces (Dassi et al. 2014). Therefore, non-manifold topology is crucial for the representation of complex geological and reservoir modelling. In this paper, the term “non-manifold” refers to non-manifold surfaces.

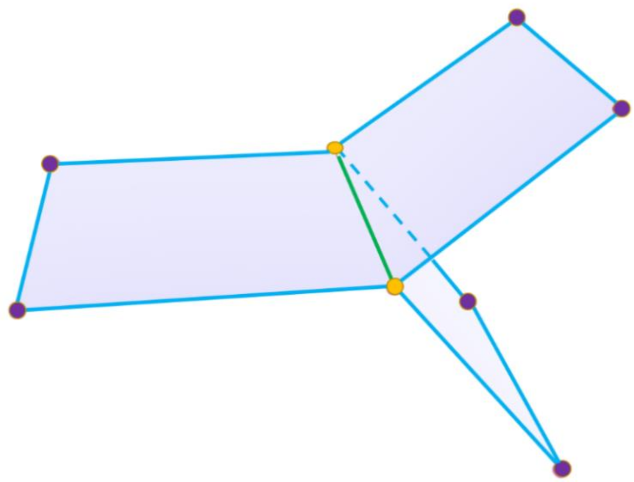

Fig.2 Three faces share one edge, a typical example of a non-manifold shape. Non-manifold vertices (yellow) and edge (green) with manifold vertices (purple) and edges (blue).

Subdivision surface algorithms cannot support non-manifold topologies. However, the support for arbitrary topologies and the other excellent features of subdivision surfaces make it worthwhile to use modified subdivision surfaces for non-manifold geological topologies. This work aims to contribute to complex geological and reservoir modelling using a non-manifold subdivision surface algorithm (surface-based geological modelling). Figure 1 represents the control mesh and the smooth surfaces of a common non-manifold geological structure by applying the non-manifold subdivision surface algorithm.

NURBS and Subdivision surfaces are also used to fit smooth surfaces with mesh or dense data (Ma et al. 2004; Panozzo et al. 2011). NURBS are primarily utilised for topologically simple cases since managing the connections between different patches of NURBS in topologically complex cases is difficult. However, the subdivision surfaces scheme generates structures with arbitrary topology and equal precision as NURBS (Ma et al. 2015). In this paper, solving the reverse problem by fitting smooth surfaces to complex geological and reservoir structures is investigated. Generated models by the non-manifold subdivision surface method are topologically similar to the initial geological structures and exploited all advantages of surface-based modelling (e.g., grid-free, smooth and controllable with some control points). Also, they have fewer vertices which can reduce the cost of processing in complex geological simulations.

It should be mentioned that the figures in this paper are rendered by Blender, which is an open-source 3D computer graphics software (http://www.blender.org/).

2 Methods

2.1 Spline surfaces

Spline surfaces are a standard method for representing high-quality free-form surfaces, which are generated by mapping from a rectangular, parametric domain (u,v) to the R^3 (x, y, z) domain. A general spline surface of bi-degree n can be obtained by

$$(u, v) \rightarrow \sum_{i=0}^{m} \sum_{j=0}^{k} c_{ij} \, N_i^n(u) N_j^n(v) \, , \tag{1}$$

where c_{ij} are the control points in R^3 and $m + 1$ and $k + 1$ are the numbers of control points in the u and v directions, respectively. Additionally, $N_i^n(u)$ and $N_i^n(v)$ are spline blending functions in the u and v directions, e.g., B-spline (basis spline) functions (Botsch et al. 2010).

NURBS (Non-Uniform Rational B-Spline) surfaces are famous spline surfaces that are useful for making high-quality, freeform and editable surfaces (Fig. 3) (Botsch et al. 2010). Theoretically, NURBS surfaces are parametric surfaces that can be made according to the numbers of weighted points (control points), parametric knot vectors and specific interpolation degrees between the control points (Piegl and Tiller, 1997).

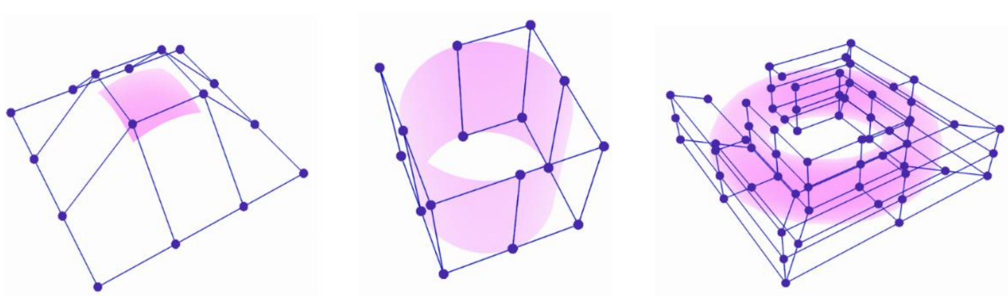

a **b** **c**

Fig. 3 Representation of the different NURBS surfaces: control mesh (blue) and NURBS surface (purple). Single NURBS surfaces are limited to topologically similar surfaces to **a** Sheet, **b** Cylinder or **c** Torus surfaces (Derose et al. 1998).

NURBS surfaces have three critical features, which are as follows:

1) B-Spline Surface: B-Spline or basis spline surfaces are piecewise parametric surfaces (see appendix 2.2) based on basis spline functions. They include control points and the surface affected by the control points.

2) Rational: This means that the control points of the B-spline have weight values that can change the effect of a control point on a surface.

3) Non-Uniform: This feature makes NURBS suitable for several practical goals (Cashman 2010). NURBS surfaces are combinations of polynomial sections joined at specific positions, which are knots (Piegl and Tiller (1997)). The knots make a surface locally modifiable while the surface remains smooth (except when the knots multiplicity increases), which means that changing the position or the weight of any specific control point can affect only the related *part* of the mesh (not the entire mesh) (Piegl and Tiller (1997)). If the knots are equally positioned, this is equivalent to a uniform B-spline. Otherwise (if the knots are arbitrarily distributed), it is a Non-Uniform B-Splines (NURBS) surface.

2.2 Limitations of NURBS surfaces

1- The main restriction of any single surface that is made up by planar parameterisation (a rectangular grid), such as NURBS, is the limitation on the construction of surfaces that are topologically similar to a sheet, cylinder or torus (Fig. 3) (Derose et al. 1998, Cashman 2010). Therefore, to create a model with a complex topology, many NURBS patches have to be smoothly connected (by stitching NURBS patches together). Multiple connections between surface patches in addition to topological or geometrical constraints make the modelling procedure more complex (Bostch et al. 2010, Cashman 2010). As a result of the strict rectangular topology of NURBS surfaces, trimming the NURBS patches before stitching is fundamental during complex shape modelling, which can create unavoidable gaps between trimmed NURBS patches (Shen et al. 2014; Sederberg et al. 2008).

2- Modifying classical NURBS surfaces, e.g., adding more control points, will influence an entire row or column of control points (Botch et al. 2010). Indeed, preserving the grid structure of NURBS surfaces during local refinement is challenging (Derose et al. 1998). It should be mentioned that T-splines, as a generalisation of the NURBS, offer local refinement and can remarkably decrease the number of control points (Sederberg et al. 2004).

2.3 Subdivision scheme

The subdivision scheme was created to overcome the difficulties of constructing smooth surfaces by supporting arbitrary topology (Zorin and Schroder 2001, Catmull and Clark 1978, Doo and Sabin 1978). The primary idea behind the subdivision scheme is to use the initial mesh to simulate a smooth structure by refinements. In practice, the modifications are carried out repeatedly until the simulated curve/ surface is fine enough. The vertices of the initial mesh (control mesh) control the shape of the final smooth structure.

Figure 4a represents a simple "control mesh", a cube with eight vertices, twelve edges and six faces. Applying the subdivision surface algorithm over the control mesh leads to the generation of the smooth mesh from the control mesh (Fig. 4b). Increasing the subdivision iteration leads to an increase in the smoothness and the number of vertices of the generated mesh (Fig. 4c). Moreover, by changing the position of the control points, the generated mesh changes smoothly (Fig. 4d).

The subdivision surfaces scheme not only overcomes the limitations of NURBS by defining smooth and controllable surfaces that need no trimming for *arbitrary topologies* but is also computationally efficient and suitable for complex geometry (Zorin 2000).

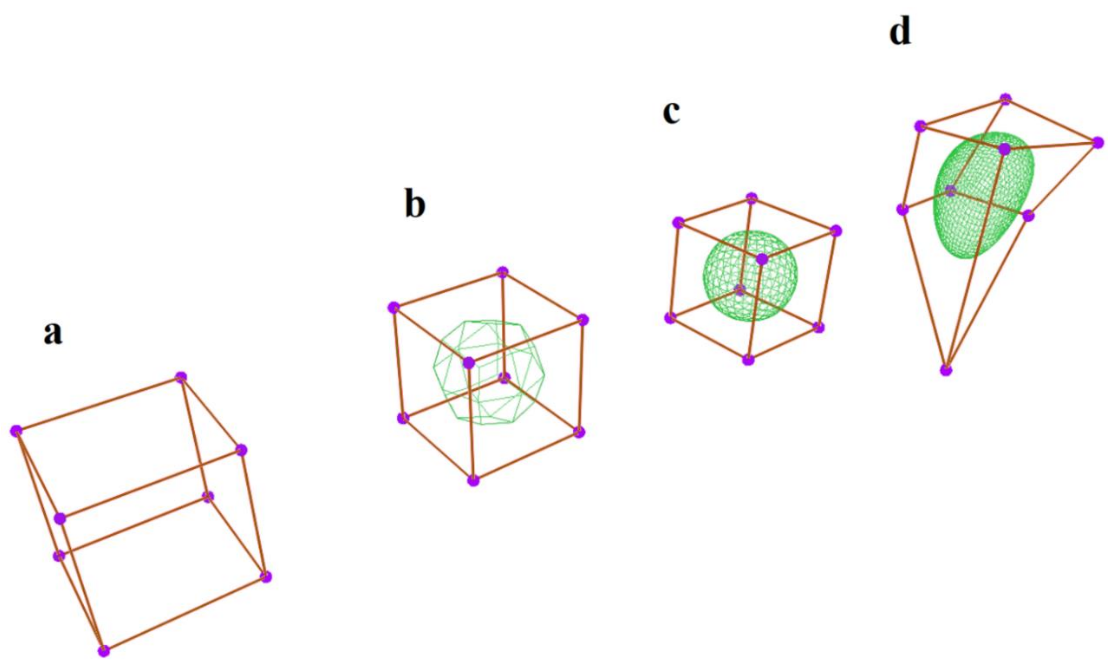

Fig.4 An example of a simple subdivision surface method, generating a smooth mesh (green edges) by regularly applying the subdivision scheme. **a** The original mesh (control mesh) has eight purple vertices (control points) and twelve red edges. **b & c** Apply the subdivision surface algorithm to the original mesh one and three times. **d**. Deformation of the resulting mesh by adapting the position of the control points

2.4 Subdivision algorithm; the combination of splitting and averaging

For generating smooth curves/surfaces in each refinement, the subdivision scheme follows two steps based on mathematical rules; **splitting** and **averaging**. In the splitting step, new vertices are inserted on the curve/surface and in the averaging step, the positions of the vertices are updated. This section explains these two steps comprehensively for generating smooth curves and surfaces, respectively.

2.4.1 Subdivision curves

The aim is to continuously refine the polygon (control mesh) to generate a smooth curve with an arbitrary degree. The vertices of the control mesh are the control points of the final smooth curve. Figure 5 shows an example of the generation of a **cubic** B-spline subdivision curve generated by a subdivision algorithm. The control mesh has four vertices (orange vertices) (Fig. 5a), and the smooth curve (purple curve) is generated after applying a subdivision refinements twice (Fig. 5b). The final curve is the combination of four curves of degree three (cubic B-splines) stitched together (Fig. 5c). By increasing the number of refinements, the final curve will be smoother, but the degree of the curves will not change. The step by step workflow for the generation of the subdivided curve is explained in the next step.

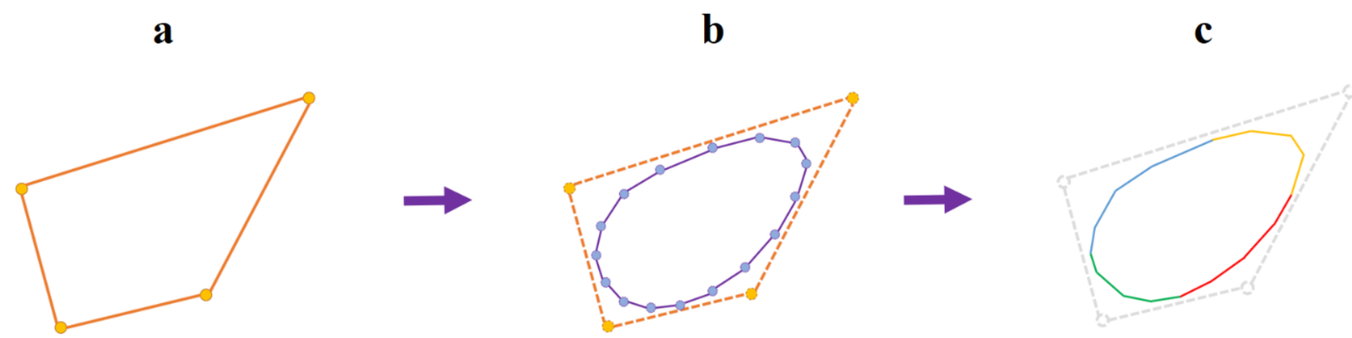

Fig. 5 Generation of a cubic B-spline subdivision curve. **a** The control mesh with four control points (orange vertices); **b** The smooth curve after two times subdivision; **c** The smooth curve is the combination of four curves (yellow, green, blue and red) of degree three.

2.4.1.1 Step by step workflow for generation of the subdivided curve

1- Splitting step: new vertices are inserted in the mid of each edge, and then the vertices are connected (Fig. 6).

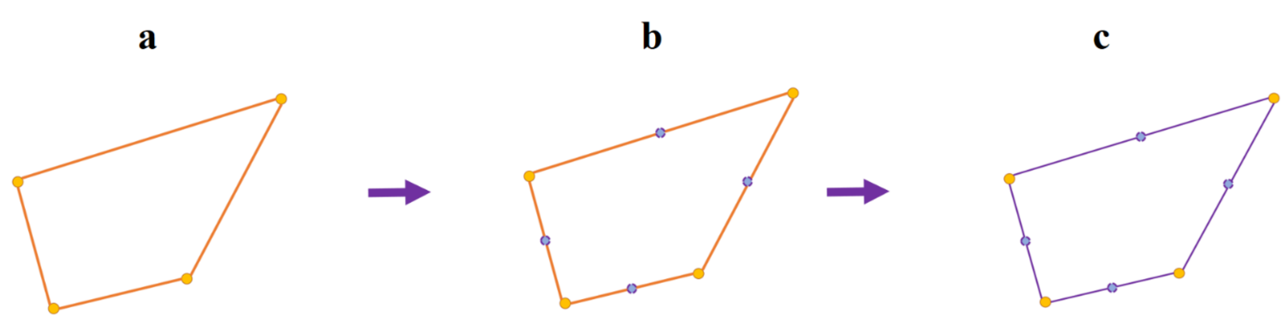

Fig. 6 Splitting step for the generation of a cubic B-spline subdivision curve. **a** The control mesh with four control points (orange vertices); **b** Inserting new vertices (purple vertices) on the mid of each edge; **c** Connecting all vertices to each other.

2- Averaging step: the location of each vertex is updated by applying the averaging mask (i.e. the new location is the weighted average of the current location of the vertex and the location of the neighbours). The averaging mask is based on the Lane-Riesenfeld algorithm (Lane and Riesenfeld 1980).

The Lane-Riesenfeld algorithm computes the averaging mask of each point of the polygon for generating B-splines of degree $n+1$ using equation (2) (Lane and Riesenfeld 1980, Vouga and Goldman 2007):

$$w = \frac{1}{2^n}\left\{ \binom{n}{0}, \binom{n}{1}, \binom{n}{2}, \ldots, \binom{n}{n} \right\}, \tag{2}$$

Where $\binom{n}{k}$ is the binominal coefficient of the n and k.

For example, Figure 7 shows the averaging step for generating the **cubic** B-splines curve. The **cubic** B-spline subdivision **mask** indicates the degree $= 3$; therefore, $n = 2$. By importing $n = 2$ into equation (2), the averaging mask for each vertex and two adjacent vertices is $= \frac{1}{4}\{1, 2, 1\}$. Therefore, the new position for each vertex (p_{new}) can be calculated by equation (3):

$$p_{new} = \frac{1}{4}(\mathbf{1} * d_1 + \mathbf{2} * p + \mathbf{1} * d_2), \tag{3}$$

where (p) is the location of the existing vertex and (d_1, d_2) are the locations of two neighbour vertices (Fig. 7c). By applying the averaging mask to all vertices of Figure 7a, the positions of all of the vertices are updated.

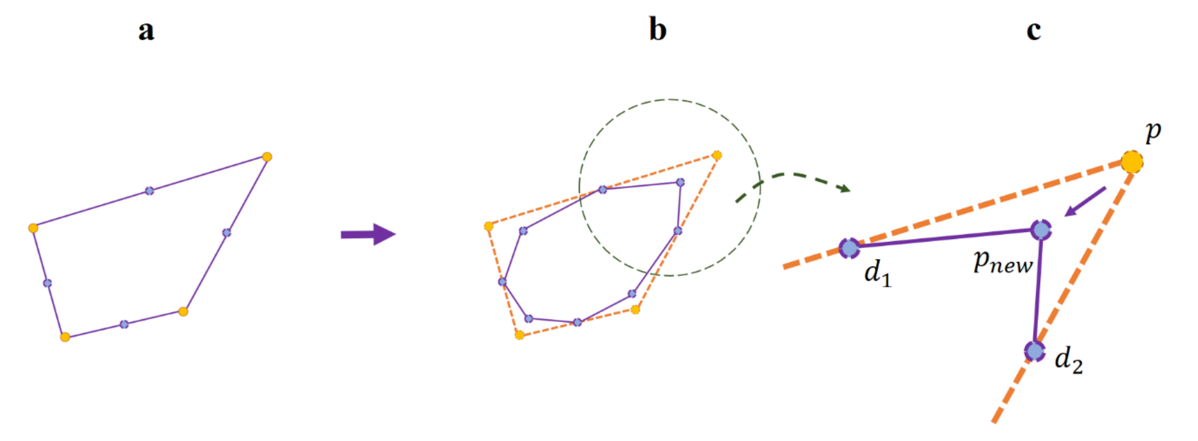

Fig. 7 Averaging step for cubic B-spline subdivision. **a** Control mesh associated with midpoint vertices (purple vertices); **b** Generating the smooth curve (purple curve) by updating the position of the all vertices based on averaging step; **c** Representation of averaging step by cubic B-spline subdivision mask

Finally, by repeatedly splitting and averaging steps (subdivision refinement), a series of smoother curves (cubic B-spline curves) will be generated (Fig. 8).

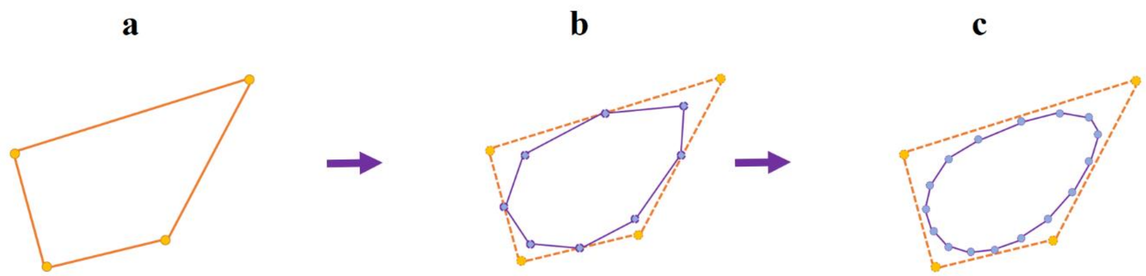

Fig. 8 Generation of cubic B-spline curves after one and two times subdivision curves. **a** Control mesh with four control points (orange vertices); **b** Generating the smooth curve (purple curve) after **one-time** subdivision curve; **c** Generated the smooth curve (purple curve) after **two times** subdivision curve.

2.4.2 Subdivision surfaces

Extending the subdivision curve approach to surfaces leads to the subdivision surface approach. Subdivision surfaces repeatedly refine the coarse mesh (control mesh) to generate a smooth surface. Similar to the subdivision curve, subdivision surfaces follow splitting and averaging steps at each refinement stage. The vertices of the control mesh are the control points of the final smooth surface. There are different subdivision surface schemes, e.g. the Catmull-Clark Scheme (Catmull and Clark 1978) for quadrilateral meshes and the Loop Scheme (Charles Loop 1987) for triangular meshes. In this section, the loop algorithm is explained. For completion, the Catmull-Clark Scheme is described in appendix 1.

2.4.2.1 Loop subdivision scheme

The Loop Scheme, defined by Charles Loop (1987), builds smooth surfaces based on triangle meshes by using splitting and averaging steps in each refinement stage.

2.4.2.2 Step-by-step workflow for the generation of the subdivided surfaces

1- Splitting step: Each triangle of the control mesh is split into four triangles by inserting a new vertex on the midpoint of each edge (Fig. 9).

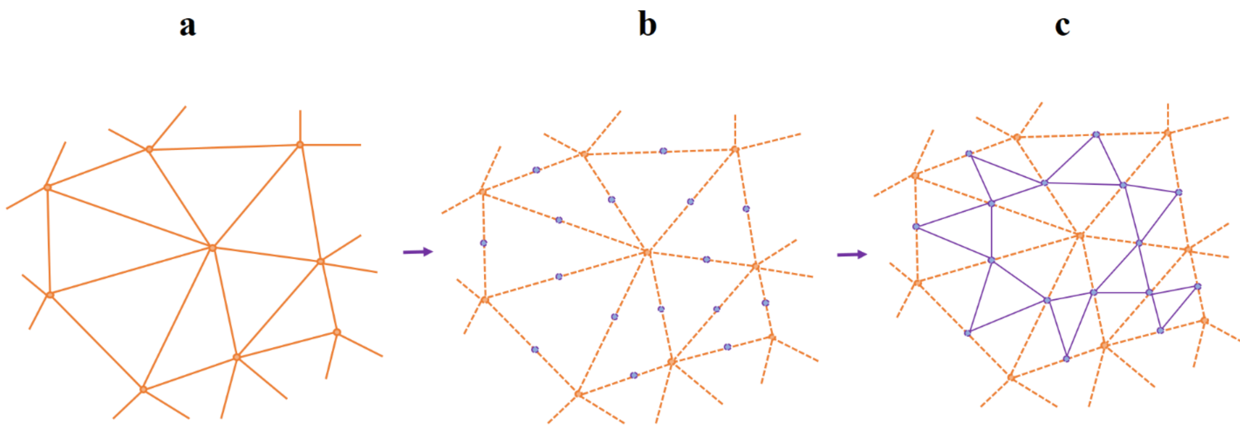

Fig. 9 Splitting step for generation of subdivision surfaces by Loop subdivision scheme. **a** The control mesh with control points (orange vertices); **b** Inserting new vertices (purple vertices) on the mid of each edge; **c** Connecting vertices to each other.

2- Averaging step: the averaging step in the Loop algorithm consists of two parts:

1. Updating the position of the new midpoint vertices generated from the splitting step (purple vertices).

2. Updating the position of the existing vertices (orange vertices).

Updating the position of the new midpoint vertices: Figure 10 shows the new midpoint (e) of an edge surrounded by four existing vertices (d_1, d_2, d_3, d_4). The Loop algorithm applies equation (4) (weighted averaging of the d_1, d_2, d_3, d_4) to determine the new location of the vertex e (Charles Loop 1987):

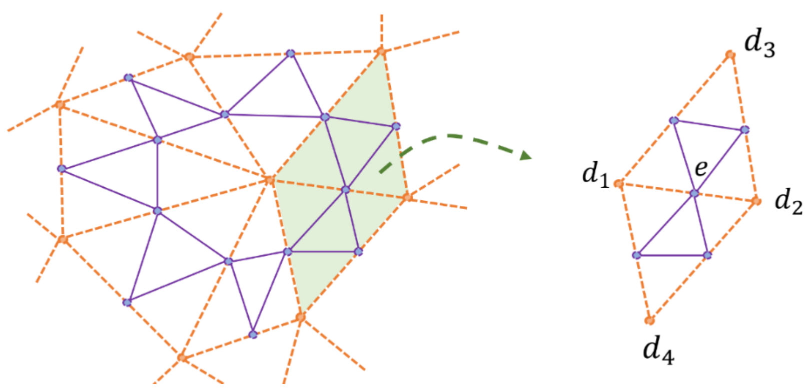

Fig. 10 Averaging step of generating the smooth surface by Loop subdivision scheme.

$$e = \frac{3}{8}(d_1 + d_2) + \frac{1}{8}(d_3 + d_4), \tag{4}$$

Updating the position of the existing vertices: Fig. 11a shows an existing vertex (v) with k adjunct vertices ($p_1, p_2, p_3, \dots, p_k$). For updating the position of the vertex (v), the Loop algorithm proposes the use of a weighted average of the vertex v and $p_1, p_2, p_3, \dots, p_k$ by equation (5) (Charles Loop 1987).

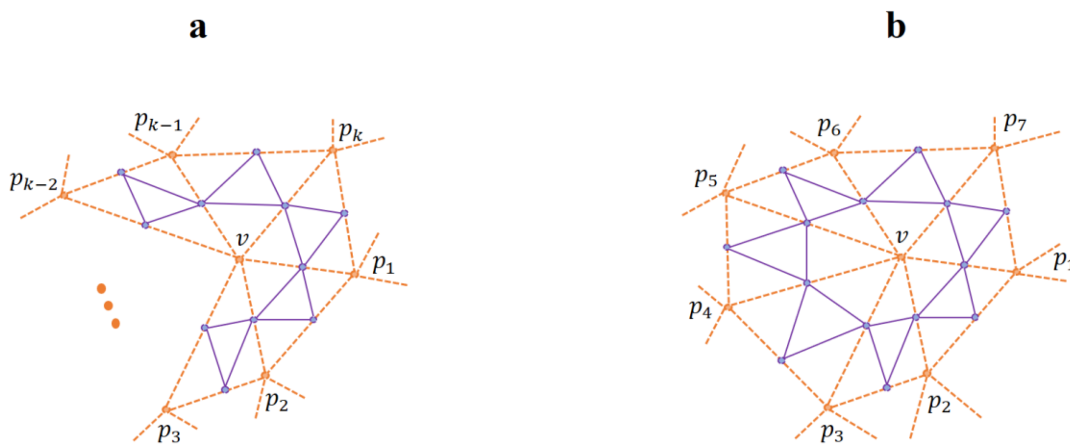

Fig. 11 Averaging step of generating the smooth surface in the Loop subdivision scheme. **a** Representation of an existing vertex (v) with k adjunct vertices. **b** The example of an existing vertex (v) with seven adjunct vertices around.

$$v_{new} = v * (1 - k\beta) + \beta \sum_1^k p_k, \quad (5)$$

where $$\beta = \frac{1}{k}\left(\frac{5}{8} - \left(\frac{3}{8} + \frac{1}{4} cos \frac{2\pi}{k}\right)^2\right), \quad (6)$$

To put it more simply, the Loop algorithm assigned the weight $(1 - k\beta)$ to the location of the existing vertex and weight β to the location of each adjacent vertex in the averaging step. For example, Fig. 11b shows the vertex v which has seven adjunct vertices and therefore, $k = 7$. Based on equation (6), $\beta = 0.049$, which means that each of the adjacent existence vertices around v has a weight = 0.049 and v has a weight = 0.65 during the averaging step.

As an alternative, Warren (1995) proposed an additional weighting scheme (equation 7) for the calculation of β when the number of adjacent vertices (k) is greater than 3 ($k > 3$).

$$\beta = \frac{3}{8k}, \quad (7)$$

By repeating the splitting and averaging steps, the final surface will be smoother, and the number of vertices will increase.

2.5 Subdivision surfaces with semi-sharp creases, A tool for modelling complex geometries

Modifying the classical subdivision algorithm allows smooth surfaces to have sharp features such as creases and corners (Derose et al. 2000, Hoppe et al. 1994). Although real-world models such as geological structures do not have entirely sharp features, managing and controlling the sharpness of creases and corners during the subdivision procedure can be very useful in building complex structures. A crease can be created on the mesh by changing the mesh shape (e.g., by applying subdivision approaches or pulling the mesh) while pinching the specific vertices or edges of the mesh (Fig. 12). With more freedom given to the related vertices or edges, the sharpness of the crease decreases.

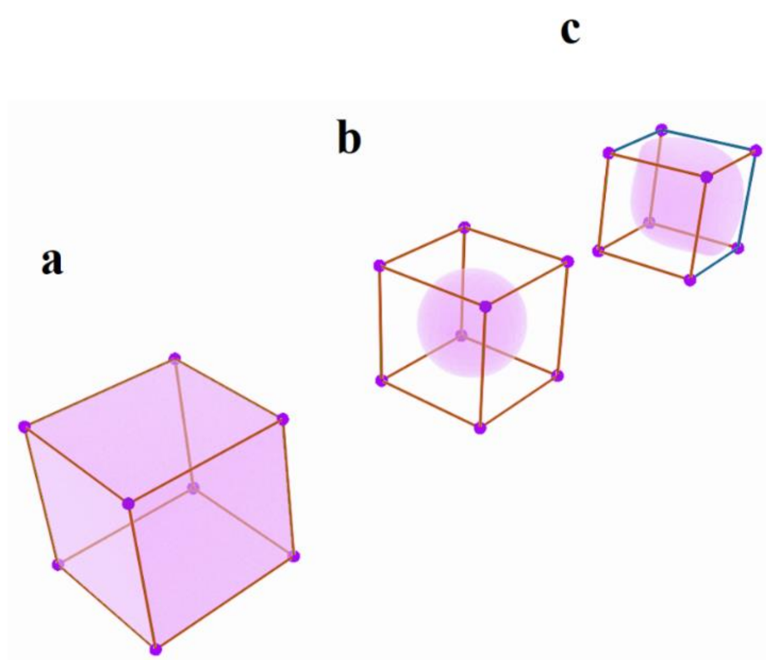

Fig. 12 Creating creases on a mesh by applying three times subdivision surfaces algorithm. **a** Control mesh. **b** All edges of the cube are smooth edges (red edges). **c** Four edges are crease edges (blue edges), and eight edges are smooth (red edges).

Practically, during the subdivision of surfaces, it is possible to consider the average crease sharpness value for each edge of the mesh. These numbers can show the resistance of the vertices of the edges to mesh modification algorithms, e.g., resistance to smoothing by subdivision surfaces (if more than one edge is connected to the vertex, the average value should be considered). The higher the crease sharpness value is, the sharper the crease. This value can be between zero and infinite, while zero indicates a smooth crease (Derose et al. 2000). Adjusting the crease sharpness allows for greater flexibility in modelling different geometric objects.

2.6 Subdivision surfaces compatible with non-manifold topologies

Classical subdivision surfaces cannot support non-manifold shapes since these shapes contain at least one local geodesic neighbourhood, which makes the topology challenging and incompatible with many methods, including subdivision surfaces (Botsch et al. 2010). In fact, some vertices and edges will not follow the classic subdivision algorithms (irregular vertices and edges). Therefore, an adapted "Non-manifold subdivision algorithm" has been proposed to combine the advantages of the subdivision surface method such as the application to arbitrary topology and still produce watertight volumes for non-manifold shapes. The *non-manifold subdivision surfaces algorithm* defined by Ying and Zorin (2001) includes several detailed rules and covers a wide range of non-manifold problems in computer graphics. In this section, the practical rules related to modelling the intersections between several surfaces, with particular interest to typical geological modelling geometries, are explained (Fig. 1 and 13). For more cases, see appendix 2 or Yian and Zorin (2001).

Figure 13 shows an example of the intersection of the surfaces. These surfaces can be different faults or intersections between a geological horizon and a fault. In this example, the edges and vertices on the shared boundary of the surfaces are non-manifold. If two non-manifold edges (blue edges) meet each other at one vertex, that vertex will be "simple non-manifold" (pink vertex); otherwise, it is "complex non-manifold" (yellow vertices).

Yian and Zorin (2001) mentioned that in the averaging step of subdivision surfaces for regular (manifold) vertices, the standard Loop algorithm should be applied. They also noted that if the vertex is simple non-manifold, the cubic B-spline subdivision algorithm (as mentioned in section 2.4) should be used, and if the vertex is complex non-manifold in most cases, a vertex will be fixed (the position of the vertex during the subdivision procedure will not be changed). Additionally, if the edge is singular (non-manifold edges, blue edges), it should be subdivided at the midpoint; otherwise, it should follow the standard Loop algorithm. For more information, see Yian and Zorin (2001). With these considerations, the representation of a wide range of non-manifold geological geometries is enabled.

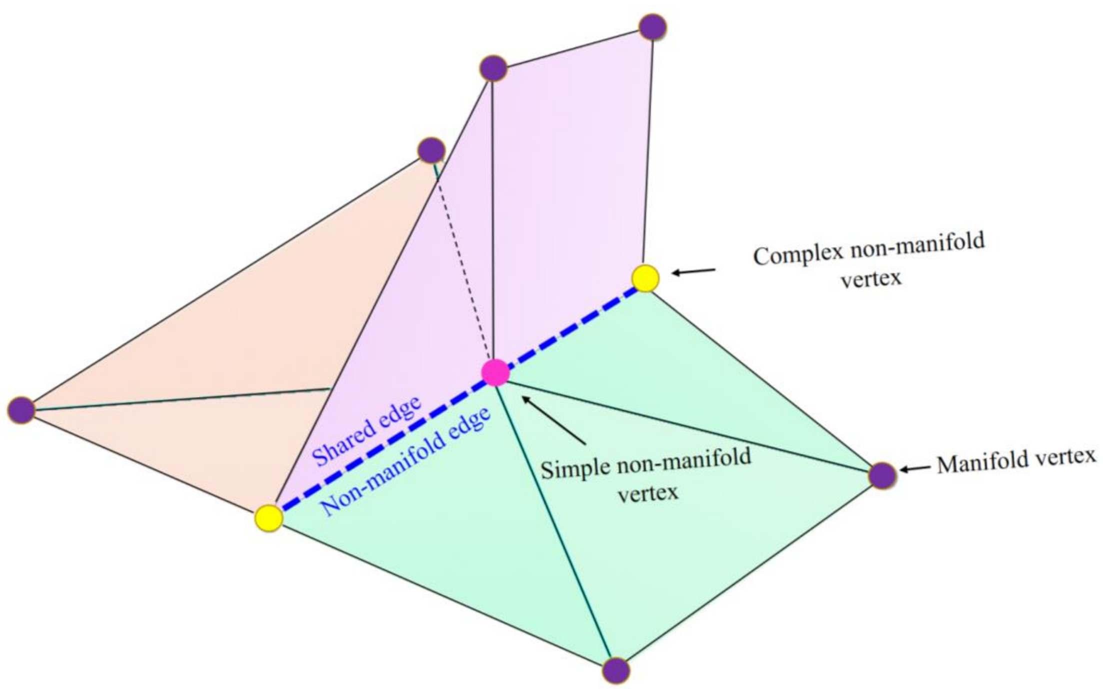

Fig. 13 Representation of Simple and complex non-manifold vertices

3. Parametric surface-based geological modelling

Caumon et al. (2004) and Jacquemyn et al. (2019) defined geological domains as closed volumes, which are mostly limited by interacting surfaces. These surfaces must represent the correct topology of the geological model and should have a watertight relationship with other surfaces. To build such closed volumes with NURBS, different NURBS surfaces (patches) are needed to interact with each other in different ways (Jacquemyn et al. 2019). Also, the relationships between independent NURBS surfaces violate geological principles, and we need to consider approaches for remedying this, such as building parametric surfaces for the entire domain and modifying the model by trimming, cutting or extrapolating the surfaces (Wellmann and Caumon 2018). As mentioned previously, according to several computer graphics references (Botsch et al. 2010, Cashman 2010, Derose et al. 1998), the need for connecting, trimming and stitching different NURBS patches to each other to build a complex model is one of the limitations of NURBS. However, the necessity for stitching and trimming separate surface patches to make watertight closed-volume surfaces is eliminated in the subdivision surface approach by building surfaces and volumes with arbitrary topology (Cashman 2010).

To build surface-based geological structures using subdivision surfaces, we propose the following steps:

1- In the first step, the control mesh is generated. The control mesh is a seamless mesh, topologically similar to the geological structure. The vertices of the control mesh are the control points of the final mesh. If the geological structure contains multiple layers or faults, the control mesh should be defined as one seamless mesh including these features.
2- Based on the geological structure, the sharpness of the crease of each edge (crease sharpness value) is specified and assigned (understanding the edges and vertices that should try to resist during classical smoothing can help in this step).
3- The non-manifold subdivision algorithm is applied, respecting the crease sharpness value of each edge.
4- If needed, the control mesh is edited by changing the positions of the control points or the crease sharpness values of the edges to reach the final goal (geological structure).
5- The steps are repeated until a final model with desired smoothness is obtained.

3.1. Different types of geological surface interactions

There are three different types of geological surface interactions that result in geological domains (Jacquemyn et al. 2019).

3.1.1 Creating closed volumes by joining surfaces at their edges

In this case, there are at least two surfaces that should be connected exactly on their edges (boundaries) to produce a watertight volume (e.g., sinuous channels, Fig. 7). Jacquemyn et al. (2019) explained how to use NURBS to build these complex shapes (Fig. 7a). In their work, two different surfaces that have exactly the same edge geometries are connected to each other. However, as mentioned previously (in section 2.2), modelling becomes more complicated by connecting (stitching) multiple NURBS patches along with topological and geometric constraints (Bostch et al. 2010, Cashman 2010). Although Jacquemyn et al. (2019) mentioned solutions such as using the degree elevation procedure or adding more control points (which is one of the limitations of classical NURBS) and Ruiu et al. (2016) suggested increasing the multiplicity of the knots (which results in reduced continuity, see Cashman, 2010), using a subdivision surface method has fewer difficulties because of its inherent features, such as supporting arbitrary topology and watertight modelling.

To build similarly closed volumes based on the subdivision surface method, at first, the seamless and similar topological mesh of the model (control mesh) is defined (Fig. 14b). In the second step, the crease sharpness values of all edges are specified. For example, in the sinuous channel case, because the top face of the channel is flat, most edges of the top face are set to fully resist smoothing during the subdivision procedure, and their crease sharpness values are set to infinite e.g., ten (blue edges). Also, most of the other edges should be smoothly subdivided; therefore, their crease sharpness values are zero (red edges). In the third step, the subdivision algorithm based on the crease sharpness value of each edge is applied with four refinement stages. The final subdivided surface is a watertight and smooth channel, which can be controlled by the control points (Fig. 14b).

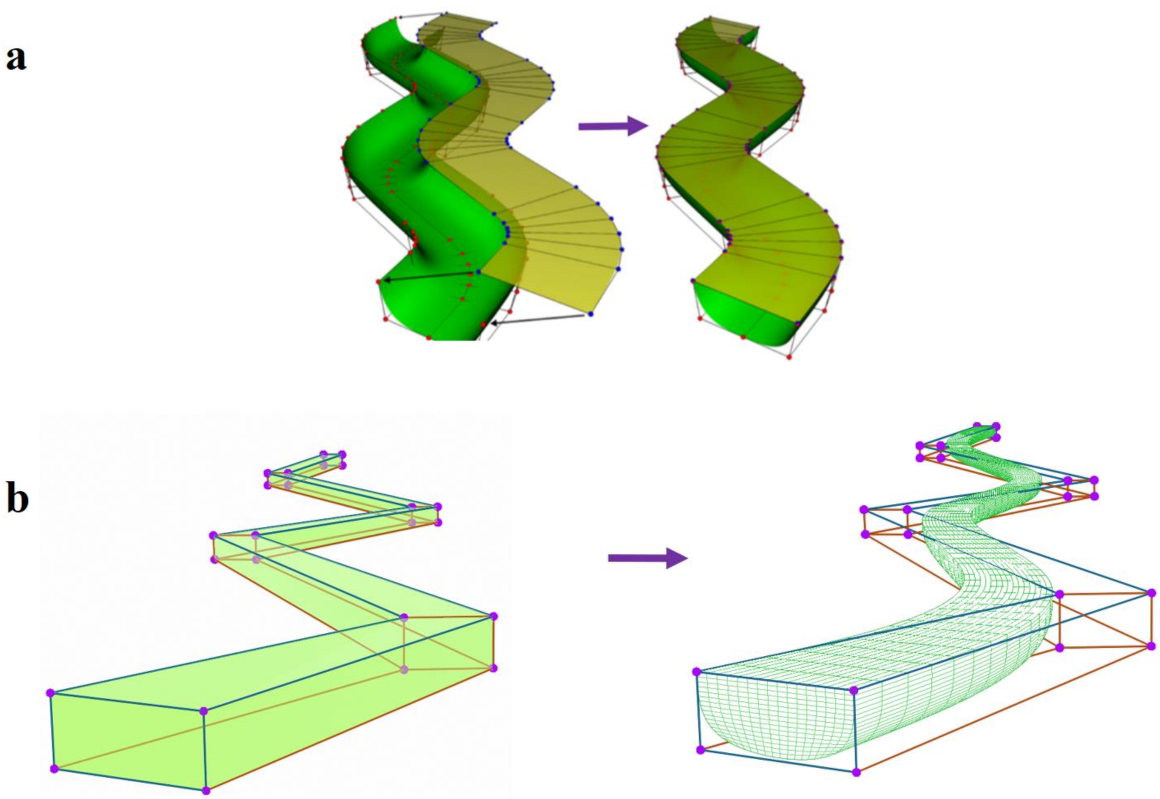

Fig. 14 Building watertight channels by NURBS (Jacquemyn et al. 2019) and subdivision surfaces (our approach). **a** Using NURBS to join surfaces at their edges to create closed volumes. **b** Building a channel using subdivision surfaces and defined crease sharpness values with subdivision stages. The crease sharpness value for each red and blue edge is zero and ten, respectively.

3.1.2 Distorted (warped) surfaces

Warped geological structures can be considered as a type of complex geological setting (in a geometric modelling sense) and are observed in nature in different ways, as described below.

Warped geological surfaces generated from geological phenomena such as folding and faulting

Warped surfaces can pose challenges in geological modelling. Since the abilities of the selected method for modelling, such as the flexibility and consistency of structures (supporting arbitrary topologies), can play an essential role in the entire modelling process, using subdivision surfaces instead of NURBS can lead to fewer difficulties, especially in layered warped structures. Fig. 15 shows a model of a faulted fold created by Catmull-Clark subdivision surfaces. Due to the suggested subdivision surfaces algorithm, the control mesh (two separate cages) is first defined (Fig. 15a). In the next step, the sharpness of the crease of each edge is assigned (the blue and red edges have crease sharpness values equal to ten and zero, respectively). Finally, the subdivision surface algorithm is applied with four stages.

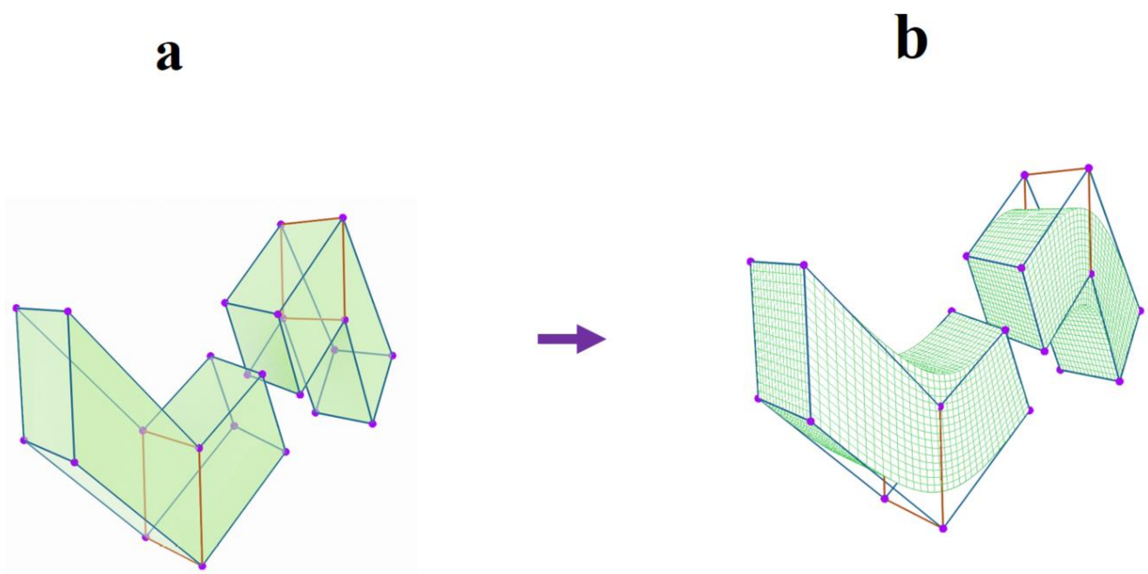

Fig. 15 An example of a faulted fold obtained through the use of subdivision surfaces. **a** During the procedure of smoothing, the sharpness of the crease value of each edge affects the mesh representation (the blue and red edges have crease sharpness values equal to ten and zero, respectively). **b** The final smooth model after applying the subdivision algorithm.

Warped geological surfaces associated with other surfaces that have geometrical connections with them

Some geological settings require the modelling of hierarchies of geometries, for example in deformed layer stacks or sedimentary sequences in a channel. Such structures can be considered through combinations of at least two NURBS surfaces with different grid structures that need to be matched (by warping one of the surfaces) to obtain the new structure. Jacquemyn et al. (2019) defined a procedure for building such structures based on NURBS. In their method, the positions of the control points of the surface to be warped need to be adapted to the parent surface(s). However, this adaption can be expensive due to the limitations of NURBS, such as the difficulties in adding more control points (as mentioned before, this is only possible by splitting parameter intervals that affect an entire row or column of the control mesh, see also Botch et al. 2010) and problems in trimming. Subdivision surface approach, unlike NURBS, first considers one comprehensive topology (control mesh) consisting of a watertight structure for both surface topologies together, the warped and parent topologies, (instead of two separate topologies) and then refine the model by assigning a specific crease sharpness value to each edge and apply the subdivision algorithm, leading to a watertight mesh with a consideration of the geometrical hierarchies.

3.1.3 Truncated hierarchically organised surfaces

An additional common geometric setting in geology is the truncation of one geological object by another object, for example along unconformities or intrusive bodies. In these cases, hierarchically organised surfaces have to be truncated against each other to obtain watertight subvolumes (surfaces that terminate on the body of another surface, e.g., clinoform surfaces). Jacquemyn et al. (2019) provide instructions to model such topologies with NURBS (e.g., model from higher hierarchal levels to lower hierarchal levels because the coordinates of lower levels are relative to higher levels; then, perform the termination operation) (Fig. 16a). However, several authors point out that using NURBS for modelling such complex structures is challenging because of the undesirable gaps arising at the boundaries between surfaces (Urick et al. 2019, Pungotra et al. 2010, Sederberg et al. 2008, Sederberg et al. 2003, Chui et al. 2000). Generally, the inherent difficulties associated with NURBS surfaces, such as limitations in stitching and problems in trimming the surfaces for building watertight volumes, complicate the entire modelling process. Also here, a modelling approach using subdivision surfaces can address this limitation. First, a simple watertight layered mesh (control mesh) is defined with a consideration of the "non-manifold topologies" (Fig. 16b). As before, crease sharpness values are assigned and a suitable subdivision surface method, now for the case of non-manifold topologies, is then to obtain the desired result.

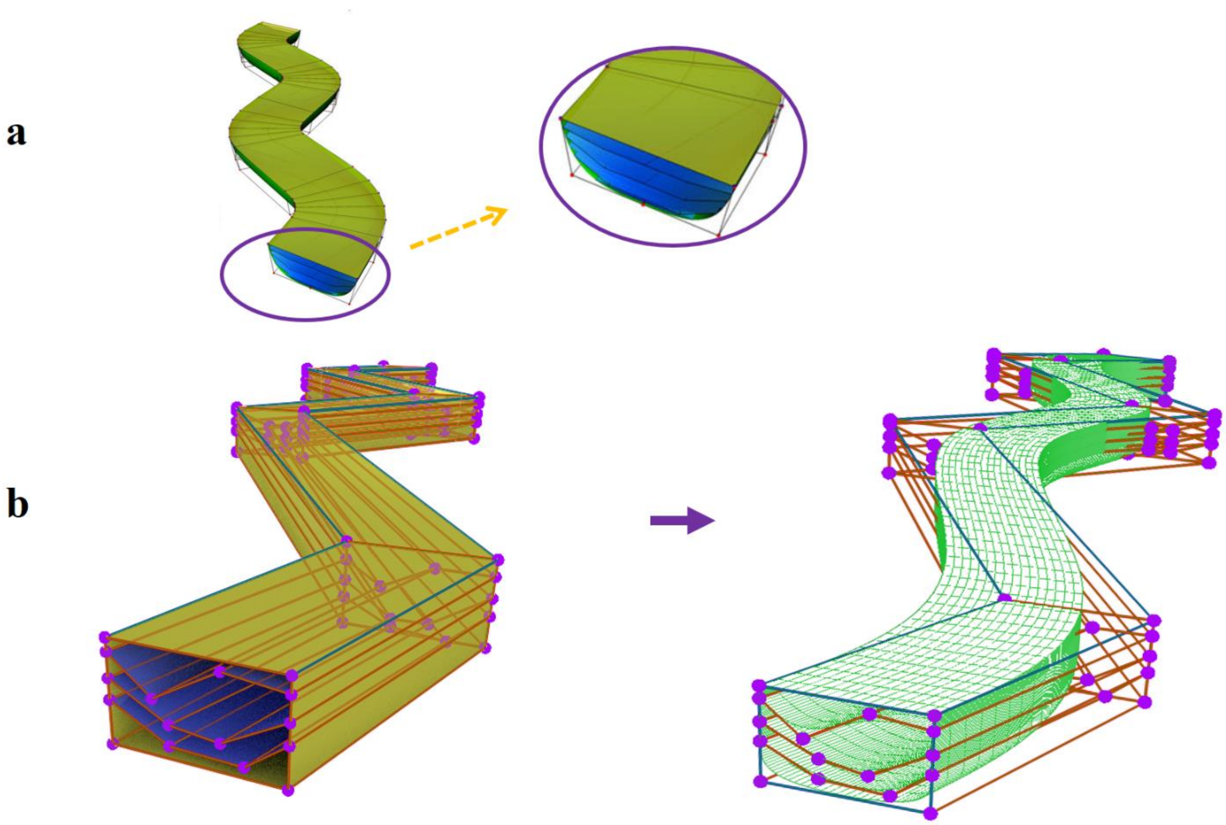

Fig. 16 a Termination of hierarchically arranged surfaces by NURBS for the basal surface of a channelised body (Jacquemyn et al. 2019). **b** Applying non-manifold Subdivision surfaces to create hierarchically arranged surfaces.

4. Surface reconstruction using the non-manifold subdivision algorithm

In addition to generating new geometric representations with the subdivision algorithm, it is also possible to obtain reconstructions of existing models – for example with the aim to obtain fully watertight meshes for further use in process simulations. This process requires specific care, as it requires matching geometric objects through adjustments of control points and crease sharpness values. We proposed therefore the following steps to achieve this aim and show the application to a geological model

4.1 Workflow for surface reconstruction

The first step is generating a suitable control mesh considering the outstanding features of the input mesh (e.g. local maxima, minima, saddle, umbilics and ridges points). The control mesh needs to have a similar topology as the target geological model, while it can be coarser with fewer vertices. The specific features should be captured by considering related parameters, e.g. principal curvatures or faces normal (Ma et al.

2015, Marinov and Kobbelt 2005, Kälberer et al. 2007). Then the surface intersections are evaluated carefully and, if necessary, additional control points are generated to support the intersections and watertight modelling. In the end, the control points are connected, which leads to the generation of the control mesh.

The second step is defining smooth parts of the model (e.g. folds) by assigning unique crease sharpness values to each edge of the control mesh, and then a suitable subdivision surface algorithm is applied to the control mesh to perform smoothing. The thirds step is fitting the watertight smooth surfaces to the input mesh. Minimising the sum of the squared distances between the vertices of the input mesh (geological structure) and the approximated mesh is a common approach for fitting a mesh (Jaimez et al. 2017, Lavoué et al. 2005, Cheng et al. 2004, Ma et al. 2002, Hoppe et al. 1994, Mallet 1997).

Assume that the geological structure (P) consists of N vertices, the control mesh (C) consists of M vertices (control points) and L edges, and the smooth surface after applying the subdivision surface algorithm t times is S. Then, the appropriate approximated surface S can be found by minimising equation (8) (Cheng et al. 2004):

$$\mathrm{E}\,(S\,) = \sum_{j=1}^{\mathrm{N}} \left\| P_j - s_q \right\|^2 , \tag{8}$$

Where s_q is the closest point of the approximated surface to the vertex j of the input mesh (P_j). The approximated surface (S) is non-linearly dependent on the positions of the control points and the crease sharpness value for each edge of the control point which convert the optimisation problem to a highly non-linear problem that can be solved using the Augmented Lagrangian method (Wu et al. 2017). For the examples presented in the following, we performed the optimization through manual adjustment. A full treatment of an automated method is beyond the scope of this paper and refer to Wu et al. (2017) for examples.

4.2 Case Study of a folded geological layer stack and an unconformity and fault

To illustrate the workflow, a folded domain with an unconformity and a fault is reconstructed by generating one comprehensive control cage and fitting the smooth surfaces by using the non-manifold subdivision surfaces method using the method described in section 4.1. The input data is a mesh of the geological structure (which can be generated by marching cubes or any other method). In this case, the input mesh is generated based on an implicit representation using the GemPy software, which is an open-source stochastic geological modelling and inversion software (De la Varga et al. 2019).

In the first step, the initial *watertight* control mesh is prepared. In the second step, the control mesh is modified by applying the non-manifold subdivision surface algorithm based on the crease sharpness value for each edge (manually assigned). Finally, the smoothed model is fitted by equation (8). The control mesh and smoothed model have been generated by the open-source python package "PySubdiv". PySubdiv is an open-source python library for non-manifold subdivision surface modelling.

In this case, the original geological structure has 26,000 vertices (Fig. 17**a**). Based on section 4.1, the control mesh consisting of only 56 control points is generated (Fig 17**b**). The control points are mainly placed on the intersecting parts of the models, e.g., the intersections between layers and faults to ensure that the final model is watertight. Also, crease sharpness values are assigned to the edges. The crease sharpness values for the edges that should create smooth surfaces (red edges) are zero, and for the edges that should be sharp (blue edges), are ten. Finally, the non-manifold subdivision surface algorithm is applied two times to the control mesh to generate a final mesh (Fig 17**c**). The final mesh has only 1,153 vertices (approximately 5% of the vertices in the original mesh).

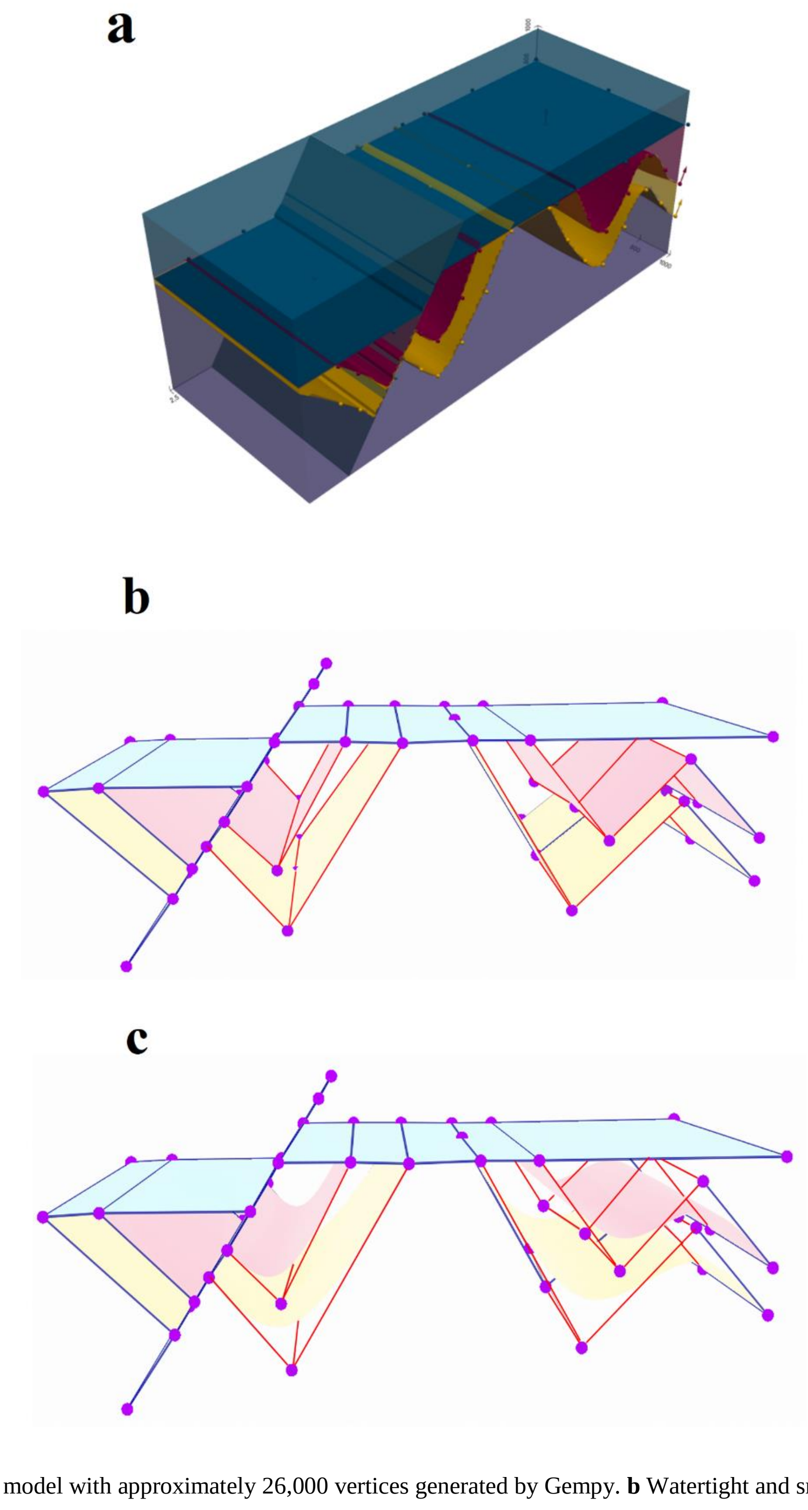

Fig. 17 a The input model with approximately 26,000 vertices generated by Gempy. **b** Watertight and smooth control mesh with 56 control points. The blue and red edges have associated crease sharpness values of ten and zero, respectively. **c** The final model with 1,153 vertices, is generated after applying two times subdivision surface algorithm generated by our method.

5 Discussions

The following section discusses the limitations and advantages of subdivision surfaces and NURBS for generating complex geological models based on three criteria: (1) accuracy in modelling the surface intersections, (2) difficulty in fitting smooth surfaces, and (3) managing control points.

5.1 Accuracy in modelling the surface intersections

In geological modelling with different scales of heterogeneity, parametric surface-based representation can preserve the accuracy of the model with less difficulty in comparison to implicit modelling approaches (Jacquemyn et al. 2019). However, classic NURBS surfaces suffer from inaccuracies from sewing multiple NURBS patches together (Cashman 2010). This feature is vital in complex geological modelling, in which the surface intersection is unavoidable e.g., in intersections of faults and horizons (Fig. 17). Sederberg et al. (2008) proposed a time-consuming three-step solution to fix the intersection of two NURBS surfaces (converting NURBS into T-splines, merging T-splines to generate a watertight surface, and then converting the merged surface into NURBS). The subdivision surface method can solve the problem during the generation of the control mesh by locating and connecting the control points at the surface intersections and then starting the procedure of smoothing and fitting (Fig. 17b). Therefore, increasing the modelling accuracy of the surface intersection is less difficult since the number of vertices of the control mesh are kept at a small value. For example, in the case study (Fig. 17), the original geological model has 26,000 vertices; however, the control mesh has just 56 vertices (control points) which are mainly located at the critical parts of the control mesh (e.g. intersection, boundary, concave and convex parts).

One important consideration is if some undesired intersections between surfaces can occur during modelling with the subdivision surface method. Most subdivision schemes (all with only positive subdivision weights) have the feature that the final subdivided surface strictly lies within the convex hull of the control mesh. Therefore, one could easily subdivide until the convex hulls are intersection-free to verify that there is no intersection. With a similar procedure, it is possible to detect intersections and resolve them. Several papers investigated the intersection aspects in subdivision surfaces (Severn and Samavati 2006, Grinspun and Schroder 2001, DeRose et al. 1998). The problem of self-intersection is also not limited to subdivision surfaces. Intersection detection has also been described and investigated comprehensively for polygonal meshes and spline surfaces (Lin and Gottschalk 1998, Hughes et al. 1996, Volino and Thalmann 1994).

5.2 Difficulty of fitting smooth surfaces

NURBS surfaces have been investigated for fitting purposes in several works with different approaches (Ma et al. 2004, Lavou'e et al. 2007). However, unlike subdivision surfaces, the majority of existing approaches using NURBS are only suitable for simple topological settings. Managing continuity conditions across neighbouring surfaces remains a demanding issue (Ma et al. 2015).

Although using subdivision surfaces can decrease the number of parameters in a subsurface model to solve inverse problems, implementing the subdivision surfaces method without paying attention to the suitable algorithm for generating a control mesh can also increase the cost of modelling. Generating a suitable control mesh as a first step for the fitting procedure by subdivision surfaces can be challenging due to the limitation of preserving the alignments and topology. Several previous works used the simplification method for generating control mesh (Hoppe et al. 1994, Suzuki et al. 1999, Kanai 2001, Panozzo et al. 2011). However, using simplifications can increase the difficulty of the fitting process by requiring geometrical optimisation (Ma et al. 2015). Also, from the geological modelling point of view, model sealing can be challenging since the horizon cutoff lines are not precisely on fault surfaces (Caumon et al. 2004). One solution would be to consider some salient features of the original mesh as the potential candidates for control points instead of simplification, e.g. Ma et al. (2015) used the umbilics and ridges as the main features of the original mesh for generating control points.

5.3 Managing control points

The grid-based structure of NURBS surfaces is restricted to a strict topology ($columns \times rows$) (Fig. 3). Therefore, the placement of control points in NURBS is less flexible than in subdivision surface methods. Subdivision surfaces are therefore a better choice to address geometric settings with complex topology. This freedom is vital in geological modelling since geologists predict the model based on real data, and the predicted model may be associated with uncertainties (Wellmann and Caumon 2018). Therefore, the model should be easily adaptable based on scientific judgment, especially by adding or deleting control points. The difficulty of adding more control points to classic NURBS structures is mentioned in several references (see section 2.2). However, unlike subdivision surfaces , NURBS surfaces support non-uniform parametrisation by knots that support a different variety of continuity (degree) of the curve or surface at any knot (Ruiu et al. 2016, Cashman 2010). Therefore, using knots inside subdivision surfaces can increase the flexibility of the control mesh. Sederberg et al. (1998) and Müller et al. (2006) generated non-uniform subdivision surfaces (NURSS) by inserting knots into the subdivision algorithm. Also, Cashman (2010) developed NURBS-compatible subdivision surfaces that refer to the NURBS surfaces without any topological constraints (the surfaces with arbitrary topology superset of the NURBS). The consideration of these method combinations in applications to geological modelling is an interesting path for further research.

6 Conclusion

NURBS and subdivision surfaces, as two main parametric surface-based representation methods in computer graphics, have also been applied successfully for geological modelling tasks before – but a detailed comparison with respect to challenging settings, such as the common case of non-manifold topologies in geological settings, was not performed. NURBS surfaces have become a standard method in CAD and they have been used successfully in explicit geological and reservoir modelling (REFS). The subdivision surface method is popular in the animation and gaming industry, but is, so far, rarely used in geological and reservoir modelling – even though it provides interesting aspects compared to NURBS. In modelling a complex structure, using NURBS is problematic because it requires a regular grid structure and a combination of several patches; therefore, special care needs to be taken in stitching and trimming these patches to obtain sealed surfaces. Subdivision surfaces, on the other hand, can more easily be adapted to support arbitrary topological structures, leading to seamless models. Understanding the similarities and differences of parametric surface-based models from a computer graphics point of view can help geological modellers make better decisions about the most suitable algorithm for different geological modelling settings.

In this paper, we placed the main emphasis also on the concept of non-manifold topology in geological and reservoir modelling. Classic subdivision scheme cannot represent non-manifold structures since these structures require more complex algorithms. Therefore, the subdivision surfaces compatible with non-manifold topologies were investigated. Additionally, subdivision surfaces were used to solve the inverse problem by generating smooth surfaces to fit the complex geological models. The final smooth structure is not only topologically similar to the geological structure but also benefits from subdivision surface advantages; e.g., it is smooth, controllable and watertight. Using the fitted models, therefore, provides more control over the model and can reduce the number of vertices for additional adaptation and optimization.

Acknowledgements We would like to thank our colleagues whose previous works motivated us to work on the topic, especially Prof. Guillaume Caumon, Dr. Pauline Collon, Prof. Leif Kobbelt, Prof. Mathew Jackson. This project has received funding from the European Institute of Innovation and Technology— Raw Materials—under grant agreements No 16258 and No 19004.

References

Botsch, M., Kobbelt, L., Pauly, M., Alliez, P., & Lévy, B. (2010). Polygon mesh processing. CRC press.

Börner, J. H., Bär, M., & Spitzer, K. (2015). Electromagnetic methods for exploration and monitoring of enhanced geothermal systems–a virtual experiment. Geothermics, 55, 78-87.

Burns, K. L. (1975). Analysis of geological events. Journal of the International Association for Mathematical Geology, 7(4), 295-321.

Cashman, T. J. (2010). NURBS-compatible subdivision surfaces (Doctoral dissertation, Cashman, Thomas J.).

Catmull, E., & Clark, J. (1978). Recursively generated B-spline surfaces on arbitrary topological meshes. Computer-aided design, 10(6), 350-355.

Caumon, G., Lepage, F., Sword, C. H., & Mallet, J. L. (2004). Building and editing a sealed geological model. Mathematical Geology, 36(4), 405-424.

Caumon, G., Collon-Drouaillet, P. L. C. D., De Veslud, C. L. C., Viseur, S., & Sausse, J. (2009). Surface-based 3D modeling of geological structures. Mathematical Geosciences, 41(8), 927-945.

Caumon, G. (2010). Towards stochastic time-varying geological modeling. Mathematical Geosciences, 42(5), 555-569.

Chatzivasileiadi, A., Wardhana, N. M., Jabi, W., Aish, R., & Lannon, S. (2018). Characteristics of 3D solid modeling software libraries for non-manifold modeling. *Computer-Aided Design and Applications*, *16*(3), 496-518.

Chen, L. Q., & Liu, D. (2012). Research on the three-dimensional geological modeling based on subdivision surface modeling technology. In Key Engineering Materials (Vol. 500, pp. 646-651). Trans Tech Publications Ltd.

Cheng, K. S., Wang, W., Qin, H., Wong, K. Y., Yang, H., & Liu, Y. (2004, October). Fitting subdivision surfaces to unorganized point data using SDM. In 12th Pacific Conference on Computer Graphics and Applications, 2004. PG 2004. Proceedings. (pp. 16-24). IEEE.

Chui, C. K., Lai, M. J., & Lian, J. A. (2000). Algorithms for G 1 connection of multiple parametric bicubic NURBS surfaces. Numerical Algorithms, 23(4), 285-313.

Corbett, P. W. M., Geiger, S., Borges, L., Garayev, M., & Valdez, C. (2012). The third porosity system understanding the role of hidden pore systems in well-test interpretation in carbonates. Petroleum Geoscience, 18(1), 73-81.

Dassi, F., Perotto, S., Formaggia, L., & Ruffo, P. (2014). Efficient geometric reconstruction of complex geological structures. Mathematics and Computers in Simulation, 106, 163-184.

De Kemp, E. A. (1999). Visualisation of complex geological structures using 3-D Bezier construction tools. Computers & Geosciences, 25(5), 581-597.

De Kemp, E. A., & Sprague, K. B. (2003). Interpretive tools for 3-D structural geological modeling part I: Bezier-based curves, ribbons and grip frames. GeoInformatica, 7(1), 55-71.

DeRose, T., Kass, M., & Truong, T. (1998, July). Subdivision surfaces in character animation. In Proceedings of the 25th annual conference on Computer graphics and interactive techniques (pp. 85-94).

Deutsch, C. V. (1997). FORTRAN Programs for Calculating Connectivity of 3-D Numerical Models and for Ranking Multiple Realizations. Submitted to Computers & Geosciences.

Deveugle, P. E., Jackson, M. D., Hampson, G. J., Farrell, M. E., Sprague, A. R., Stewart, J., & Calvert, C. S. (2011). Characterisation of stratigraphic architecture and its impact on fluid flow in a fluvial-dominated deltaic reservoir analog: Upper Cretaceous Ferron Sandstone Member, Utah. AAPG bulletin, 95(5), 693-727.

Doo, D., & Sabin, M. (1978). Behaviour of recursive division surfaces near extraordinary points. Computer-Aided Design, 10(6), 356-360.

Estellers, V., Schmidt, F., & Cremers, D. (2018, September). Robust Fitting of Subdivision Surfaces for Smooth Shape Analysis. In 2018 International Conference on 3D Vision (3DV) (pp. 277-285). IEEE.

Fisher, T. R., & Wales, R. Q. (1992). Three dimensional solid modeling of geo-objects using Non-Uniform Rational B-Splines (NURBS). In Three-dimensional modeling with geoscientific information systems (pp. 85-105). Springer, Dordrecht.

Florez, H., Manzanilla-Morillo, R., Florez, J., & Wheeler, M. F. (2014). Spline-based reservoir's geometry reconstruction and mesh generation for coupled flow and mechanics simulation. Computational Geosciences, 18(6), 949-967.

Geiger, S., & Matthäi, S. (2014). What can we learn from high-resolution numerical simulations of single-and multi-phase fluid flow in fractured outcrop analogues?. Geological Society, London, Special Publications, 374(1), 125-144.

Gjøystdal, H., Reinhardsen, J. E., & Åstebøl, K. (1985). Computer representation of complex 3-D geological structures using a new "solid modeling" technique. Geophysical Prospecting, 33(8), 1195-1211.

Graham, G. H., Jackson, M. D., & Hampson, G. J. (2015). Three-dimensional modeling of clinoforms in shallow-marine reservoirs: Part 1. Concepts and application. AAPG Bulletin, 99(6), 1013-1047.

Grinspun, E., & Schroder, P. (2001, October). Normal bounds for subdivision-surface interference detection. In Proceedings Visualization, 2001. VIS'01. (pp. 333-570). IEEE.

Hassanpour, M. M., Pyrcz, M. J., & Deutsch, C. V. (2013). Improved geostatistical models of inclined heterolithic strata for McMurray Formation, Alberta, Canada. AAPG bulletin, 97(7), 1209-1224.

Hoppe, H., DeRose, T., Duchamp, T., Halstead, M., Jin, H., McDonald, J., ... & Stuetzle, W. (1994, July). Piecewise smooth surface reconstruction. In Proceedings of the 21st annual conference on Computer graphics and interactive techniques (pp. 295-302).

Hughes, M., DiMattia, C., Lin, M. C., & Manocha, D. (1996, June). Efficient and accurate interference detection for polynomial deformation. In Proceedings Computer Animation'96 (pp. 155-166). IEEE.

Jackson, M. D., Hampson, G. J., Saunders, J. H., El-Sheikh, A., Graham, G. H., & Massart, B. Y. G. (2014). Surface-based reservoir modelling for flow simulation. Geological Society, London, Special Publications, 387(1), 271-292.

Jacquemyn, C., Melnikova, Y., Jackson, M. D., Hampson, G. J., & John, C. M. (2016, August). Geologic modelling using parametric nurbs surfaces. In ECMOR XV-15th European Conference on the Mathematics of Oil Recovery (pp. cp-494). European Association of Geoscientists & Engineers.

Jacquemyn, C., Jackson, M. D., & Hampson, G. J. (2019). Surface-based geological reservoir modelling using grid-free NURBS curves and surfaces. Mathematical Geosciences, 51(1), 1-28.

Jaimez, M., Kerl, C., Gonzalez-Jimenez, J., & Cremers, D. (2017, May). Fast odometry and scene flow from RGB-D cameras based on geometric clustering. In 2017 IEEE International Conference on Robotics and Automation (ICRA) (pp. 3992-3999). IEEE.

Jones, C. B. (1989). Data structures for three-dimensional spatial information systems in geology. International Journal of Geographical Information System, 3(1), 15-31.

Kanai, T. (2001, November). MeshToSS: Converting Subdivision Surfaces from Dense Meshes. In VMV (pp. 325-332).

Kälberer, F., Nieser, M., & Polthier, K. (2007, September). Quadcover-surface parameterisation using branched coverings. In Computer graphics forum (Vol. 26, No. 3, pp. 375-384). Oxford, UK: Blackwell Publishing Ltd.

Lavoué, G., Dupont, F., & Baskurt, A. (2005, June). Subdivision surface fitting for efficient compression and coding of 3D models. In Visual Communications and Image Processing 2005 (Vol. 5960, p. 59603F). International Society for Optics and Photonics.

Lavoué, G., Dupont, F., & Baskurt, A. (2007, March). A framework for quad/triangle subdivision surface fitting: Application to mechanical objects. In Computer Graphics Forum (Vol. 26, No. 1, pp. 1-14). Oxford, UK: Blackwell Publishing Ltd.

Lin, M., & Gottschalk, S. (1998, May). Collision detection between geometric models: A survey. In Proc. of IMA conference on mathematics of surfaces (Vol. 1, No. 602-608, p. 31).

Loop, C. (1987). Smooth subdivision surfaces based on triangles. Master's thesis, University of Utah, Department of Mathematics.

Ma, W., Ma, X., Tso, S. K., & Pan, Z. (2002, July). Subdivision surface fitting from a dense triangle mesh. In Geometric Modeling and Processing. Theory and Applications. GMP 2002. Proceedings (pp. 94-103). IEEE.

Ma, X., Keates, S., Jiang, Y., & Kosinka, J. (2015). Subdivision surface fitting to a dense mesh using ridges and umbilics. Computer Aided Geometric Design, 32, 5-21.

Mallet, J. L. (1997). Discrete modeling for natural objects. Mathematical geology, 29(2), 199-219.

Marinov, M., & Kobbelt, L. (2005). Optimisation methods for scattered data approximation with subdivision surfaces. Graphical Models, 67(5), 452-473.

Müller, K., Reusche, L., & Fellner, D. (2006). Extended subdivision surfaces: Building a bridge between NURBS and Catmull-Clark surfaces. ACM Transactions on Graphics (TOG), 25(2), 268-292.

Paluszny, A., Matthäi, S. K., & Hohmeyer, M. (2007). Hybrid finite element–finite volume discretisation of complex geologic structures and a new simulation workflow demonstrated on fractured rocks. Geofluids, 7(2), 186-208.

Piegl L, Tiller W (1997) The NURBS book. Monographs in visual communications, 2nd edn. Springer,

Pungotra, H., Knopf, G. K., & Canas, R. (2010). Merging multiple B-spline surface patches in a virtual reality environment. Computer-Aided Design, 42(10), 847-859.

Pyrcz, M. J., Boisvert, J. B., & Deutsch, C. V. (2009). ALLUVSIM: A program for event-based stochastic modeling of fluvial depositional systems. Computers & Geosciences, 35(8), 1671-1685.

Rossignac, J., & Cardoze, D. (1999, June). Matchmaker: Manifold Breps for non-manifold r-sets. In Proceedings of the fifth ACM symposium on Solid modeling and applications (pp. 31-41).

Ruiu, J., Caumon, G., & Viseur, S. (2016). Modeling channel forms and related sedimentary objects using a boundary representation based on non-uniform rational B-splines. Mathematical Geosciences, 48(3), 259-284.

Sederberg, T. W. (1985). Piecewise algebraic surface patches. Computer Aided Geometric Design, 2(1-3), 53-59.

Sederberg, T. W., Zheng, J., Bakenov, A., & Nasri, A. (2003). T-splines and T-NURCCs. ACM transactions on graphics (TOG), 22(3), 477-484.

Sederberg, T. W., Cardon, D. L., Finnigan, G. T., North, N. S., Zheng, J., & Lyche, T. (2004). T-spline simplification and local refinement. ACM transactions on graphics (TOG), 23(3), 276-283.

Sederberg, T. W., Finnigan, G. T., Li, X., Lin, H., & Ipson, H. (2008). Watertight trimmed NURBS. ACM Transactions on Graphics (TOG), 27(3), 1-8.

Severn, A., & Samavati, F. (2006, May). Fast intersections for subdivision surfaces. In International Conference on Computational Science and Its Applications (pp. 91-100). Springer, Berlin, Heidelberg

Shen, J., Kosinka, J., Sabin, M. A., & Dodgson, N. A. (2014). Conversion of trimmed NURBS surfaces to Catmull–Clark subdivision surfaces. Computer Aided Geometric Design, 31(7-8), 486-498.

Sprague, K. B., & De Kemp, E. A. (2005). Interpretive tools for 3-D structural geological modelling part II: Surface design from sparse spatial data. GeoInformatica, 9(1), 5-32.

Suzuki, H., Takeuchi, S., & Kanai, T. (1999, October). Subdivision surface fitting to a range of points. In Proceedings. Seventh Pacific Conference on Computer Graphics and Applications (Cat. No. PR00293) (pp. 158-167). IEEE.

Thiele, S. T., Jessell, M. W., Lindsay, M., Ogarko, V., Wellmann, J. F., & Pakyuz-Charrier, E. (2016). The topology of geology 1: Topological analysis. Journal of Structural Geology, 91, 27-38.

Urick, B., Marussig, B., Cohen, E., Crawford, R. H., Hughes, T. J., & Riesenfeld, R. F. (2019). Watertight Boolean operations: A framework for creating CAD-compatible gap-free editable solid models. Computer-aided design, 115, 147-160.

de la Varga, M., Schaaf, A., & Wellmann, F. (2019). GemPy 1.0: open-source stochastic geological modeling and inversion. Geoscientific Model Development.

Volino, P., & Thalmann, N. M. (1994, August). Efficient self-collision detection on smoothly discretised surface animations using geometrical shape regularity. In Computer graphics forum (Vol. 13, No. 3, pp. 155-166). Edinburgh, UK: Blackwell Science Ltd.

Vouga, E., & Goldman, R. (2007). Two blossoming proofs of the Lane-Riesenfeld algorithm. Computing, 79(2), 153-162.

Wellmann, F., & Caumon, G. (2018). 3-D Structural geological models: Concepts, methods, and uncertainties. In Advances in Geophysics (Vol. 59, pp. 1-121). Elsevier.

Wu, X., Zheng, J., Cai, Y., & Li, H. (2017). Variational reconstruction using subdivision surfaces with continuous sharpness control. Computational Visual Media, 3(3), 217-228.

Ying, L., & Zorin, D. (2001, October). Non-manifold subdivision. In Proceedings Visualization, 2001. VIS'01. (pp. 325-569). IEEE.

Zehner, B., Börner, J. H., Görz, I., & Spitzer, K. (2015). Workflows for generating tetrahedral meshes for finite element simulations on complex geological structures. Computers & Geosciences, 79, 105-117.

Zhang, X., Pyrcz, M. J., & Deutsch, C. V. (2009). Stochastic surface modeling of deepwater depositional systems for improved reservoir models. Journal of Petroleum Science and Engineering, 68(1-2), 118-134.

Zorin, D. (2000). Subdivision for modeling and animation. SIGGRAPH2000 course notes.

Zorin, D., & Schröder, P. (2001). A unified framework for primal/dual quadrilateral subdivision schemes. Computer Aided Geometric Design, 18(5), 429-454.

Appendix

1. Catmull-Clark subdivision scheme

The Catmull-Clark algorithm was first defined in 1978 by Edwin Catmull and Jim Clark (Catmull and Clark 1978). This scheme is a type of approximation approach and can be applied to quadrilateral meshes. This scheme follows two steps (similar to the loop scheme): first, generate new vertices (splitting step), and then compute the new location of all vertices (averaging step).

Generating the new vertices includes two parts: first, create a face point for each face (f), and second, make an edge point (e) on each edge (Fig. 18) (Catmull and Clark 1978).

1) Each face has a face point (f)

$$\mathrm{f} = \frac{1}{4}\sum_{k=1}^{4} \mathrm{d}_k \ , \tag{9}$$

2) Each interior edge has an edge point (e)

$$e = \frac{1}{16}(d_5 + d_6 + 6 * d_7 + 6 * d_8 + d_9 + d_{10}) \ , \tag{10}$$

In the averaging step, the location of the vertex v will be updated based on the face points (f_i) and edge points (e_i) around v by equation (10) of Catmull and Clark (1978)

$$v_{new} = \frac{n-3}{n} * v + \frac{2}{n} * L + \frac{1}{n} * T, \tag{11}$$

where n is the number of face points or edge points around v and

$$L = \frac{1}{n}\sum_{i=1}^{n} \mathrm{e}_i \,, \tag{12}$$

$$T = \frac{1}{n}\sum_{i=1}^{n} \mathrm{f}_i \,, \tag{13}$$

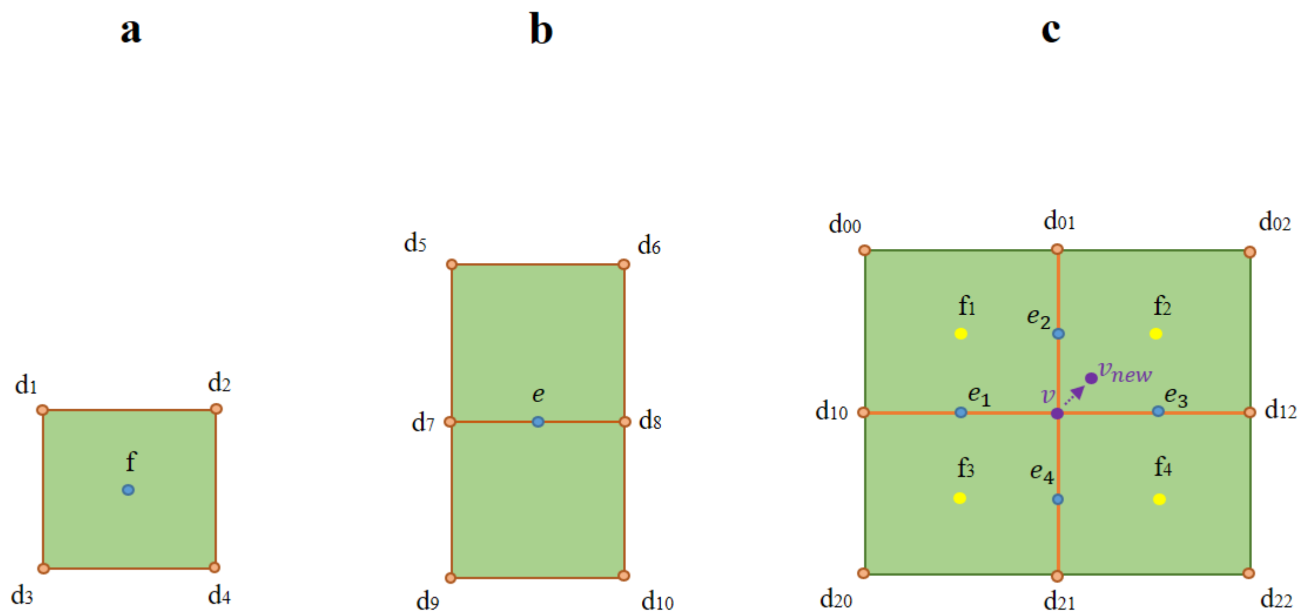

Fig. 18 Catmull-Clark subdivision scheme. **a** Finding the face point for each face. **b** Finding the edge point for each interior edge. **c** Computing the new position of vertex v based on the neighbourhood face and edge points.

2. Non-manifold subdivision surfaces algorithm

Ying and Zorin (2001) defined the extended Loop subdivision algorithm to model non-manifold structures, which is as follows:

T(v) is considered the set of all triangles of the mesh around vertex v (Fig. 19). Based on the definition in the previous section, vertex v is a *manifold vertex* if **two** favourite sequential triangles are inside T(v) and share one edge connected to v. This vertex can be either inside (interior vertex) or a boundary vertex. Additionally, an edge is named a *manifold edge* if it is shared by **two** triangles of the mesh (the manifold edge can be part of just one triangle if the edge is a boundary edge).

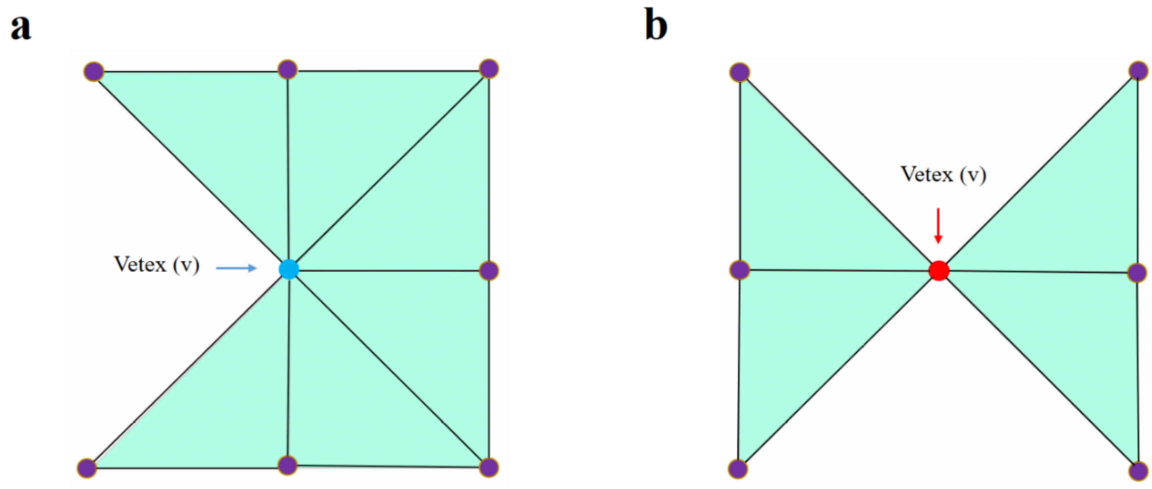

Fig. 19 Representation of T(v) (a set of triangles) around vertex v (center vertex). **a** Representation of a manifold vertex v (blue vertex); two favourite sequential tringles inside T(v) share one edge connected to v. **b** Representation of a non-manifold vertex v (red vertex).

A non-manifold vertex and edge are named a singular vertex and edge, respectively. Considering M(v) as the largest set of triangles inside T(v) which consists of the specific triangles such that every pair of favourite sequential triangles around v share an edge (Fig. 20 shows T(v), which consist of $M_1(v)$ and $M_2(v)$). It should be mentioned that the sets of triangles inside each M(v) can be either manifold or non-manifold. Also, non-manifold sets of triangles can be split into manifold sets. Therefore, each M(v) can be considered a combination of *manifold* segments, which are called Q(v); e.g., $M_1(v)$ and $M_2(v)$ consist of one and three Q(v), respectively. Indeed, Q(v) (the *manifold* set of triangles around v) is the largest set of triangles such that all two sequential triangles of it share a *manifold* edge.

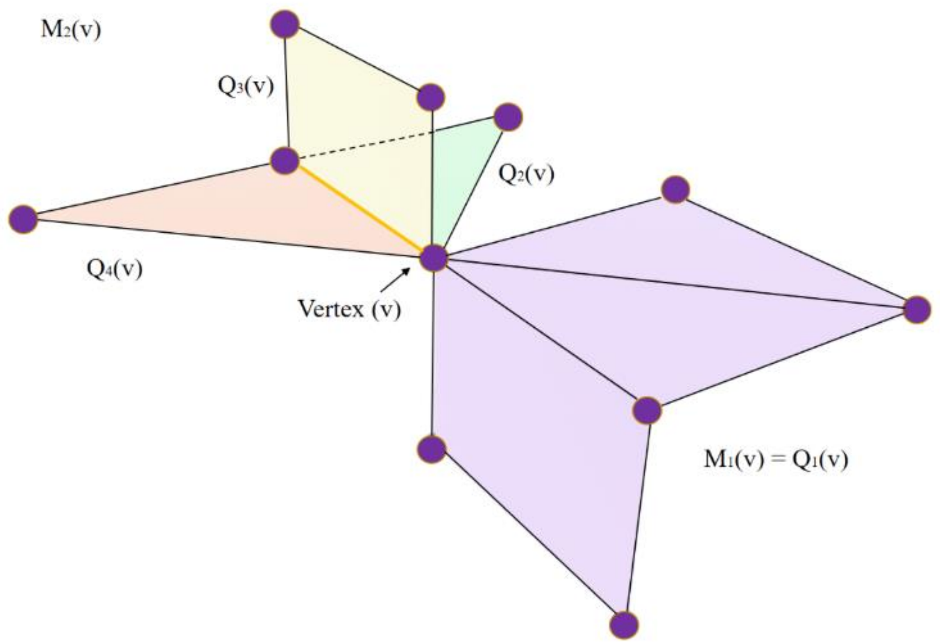

Fig. 20 T(v) consists of two parts (M_1(v) and M_2(v)); M_2(v) includes three-manifold parts, Q_2(v), Q_3(v) and Q_4(v), and M_1(v) has one manifold part, Q_1(v). The yellow edge represents the non-manifold edge which is shared between three edges.

The singular vertex v is "simple" when it is part of a single M(v), and two singular edges should meet each other at v (all of the $Q_{(v)}$-manifold regions around v share edges); otherwise, it is a "complex" singular vertex (Fig. 21). For regular vertices, the standard Loop algorithm should be used. If the vertex is simple singular, the cubic B-spline subdivision algorithm (as mentioned in section 2.4) should be used. Otherwise, the vertex is complex singular, and in most cases, a vertex can be fixed. Additionally, if the edge is singular, it should be subdivided at the midpoint, and if it is not singular, it should generally follow the regular Loop algorithm. For more information, please check Yian and Zorin (2001).

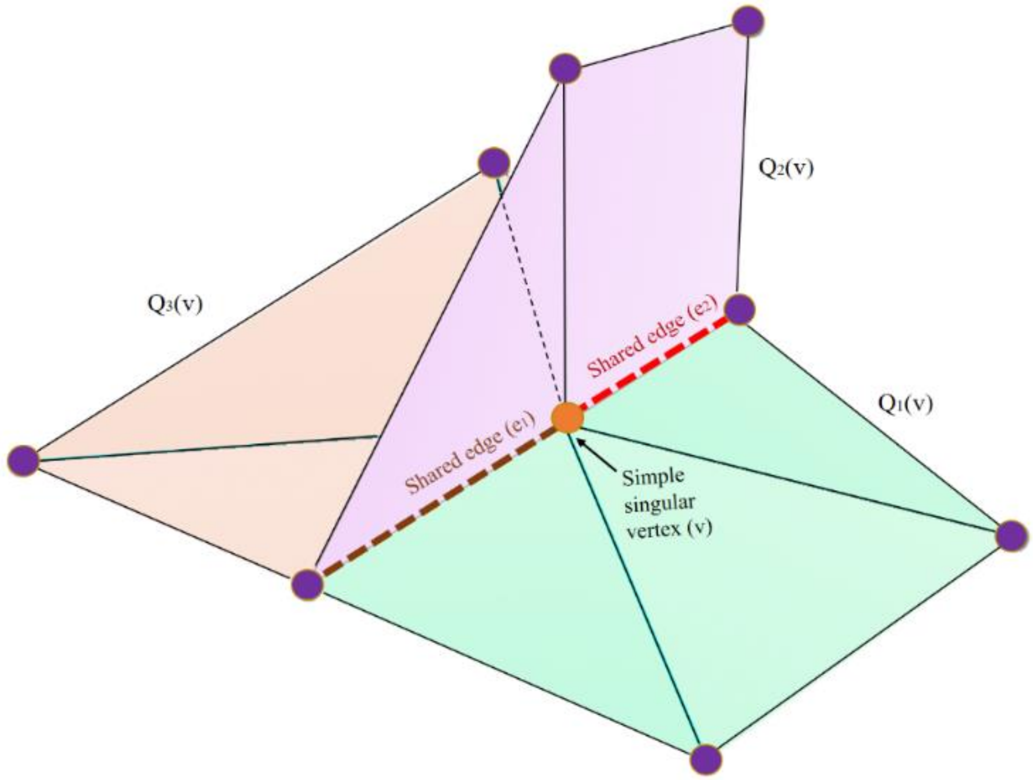

Fig. 21 Simple singular vertex (v) (orange vertex)